scientific reports

Check for updates

OPEN

Elevated SGO2 expression in lung adenocarcinoma promotes migration and invasion via MAD2 and correlates with poor prognosis

Min Sun[1], Wenzheng Zhou[1], Guohao Wei[1], Mengyao Lv[1], Yan Sun[2], Huihui Zhao[1]✉ & Chuandong Zhu[1]✉

Lung adenocarcinoma is a globally prevalent malignant tumor with a high death rate, notorious for its invasive and metastatic capabilities. SGO2 is a key protein in the cell division process, influencing the development of various malignant tumors. However, research on the biological functions of SGO2 in Lung adenocarcinoma remains limited. By utilizing the Cancer Genome Atlas (TCGA) database, we performed an analysis of SGO2 expression levels in a cohort comprising 206 Lung adenocarcinoma patients in comparison to 200 non-neoplastic control specimens. Subsequently, we validated our findings through immunohistochemical staining in a subset of 21 Lung adenocarcinoma cases from Nanjing Second Hospital. Furthermore, the functional role of SGO2 in the H1299 cell line was assessed through a series of experiments including Western blotting, CCK-8 assays, Transwell assays for invasion, wound healing assays, and flow cytometric analysis. The study also explored the influence of SGO2 on the regulation of MAD2 expression. The enhancement of SGO2 expression in Lung adenocarcinoma tissues was significantly associated with a poor prognosis in patients. A reduction in SGO2 expression markedly decreased the proliferative, migratory, and invasive capabilities of H1299 cells, a phenomenon that may be attributed to the regulation of MAD2 expression by SGO2. SGO2 exerted a pivotal influence on the metastatic behavior of Lung adenocarcinoma cells by governing the expression of MAD2, thereby contributing substantially to the molecular pathogenesis of Lung adenocarcinoma.

Keywords SGO2, MAD2, Lung Adenocarcinoma, Prognosis, Migration, Invasion

Arising from the epithelial lining of the respiratory tract, lung cancer represents a malignant form of neoplasia[1]. The persistently high incidence and mortality rates of this disease pose significant challenges to global public health[2,3]. Lung adenocarcinoma (LUAD) is the most commonly encountered subtype within the classifications of non-small cell lung cancer (NSCLC)[4].Characterized by its invasive and metastatic nature, LUAD exhibits a notably poor prognosis, with a post-surgical five-year survival rate falling under 50% for early-stage patients[5,6]and precipitously declining to a range of only 4% to 15% for those with advanced-stage disease[7,8]. It is particularly concerning that LUAD often remains undetected until it has progressed to an advanced stage[9], a phase where conventional chemotherapeutic and radiotherapeutic approaches offer limited benefit and fail to substantially impact prognosis.Hence, it is imperative to uncover novel prognostic biomarkers and investigate the underlying molecular pathways to facilitate the advancement of targeted therapeutic strategies for lung cancer. One protein that has increasingly attracted interest due to its significant function in cell cycle regulation and chromosome separation is Shugoshin 2 (SGO2). The burgeoning focus on SGO2 reflects its potential as a key element in the pursuit of more effective treatments. As part of the Shugoshin protein family, SGO2 is crucial for ensuring the fidelity of chromosome distribution during the process of cell division, exerting a substantial influence on the proper functioning of cells[10].The precise segregation of chromosomes during both mitosis and meiosis is essential for the consistent replication and passage of the genome[11]. SGO2 is crucial for upholding normal physiological states, and any dysregulation in its expression may trigger the development of numerous ailments. Research has demonstrated that SGO2 is closely associated with tumor progression. In

[1]Department of Oncology, The Second Hospital of Nanjing, Nanjing University of Chinese Medicine, Nanjing 210003, China. [2]Department of Medical Oncology, Jiangsu Cancer Hospital, Nanjing Medical University, Nanjing 210009, China. ✉email: Zhaohh1981@njucm.edu.cn; zhucd@njucm.edu.cn

hepatocellular carcinoma, SGO2 expression has been shown to be significantly upregulated, promoting cancer progression by manipulating various cellular activities encompassing growth, programmed cell death, and metastatic potential[12,13]. Inhibition of RAB1A ubiquitination by SGO2 has been implicated in facilitating the progression of prostate cancer, leading to increased cellular proliferation and metastasis[14]. Moreover, elevated expression levels of SGO2 have been observed in gliomas, indicating a correlation with the progression of this malignancy[15]. On a related note, MAD2 assumes a critical role within the Spindle Assembly Checkpoint (SAC) complex, ensuring the fidelity of chromosome alignment during metaphase[16]. The interaction between SGO2 and MAD2 during the separation of sister chromatids suggests a cooperative mechanism through which these proteins modulate the mitotic process in eukaryotic cells[17]. Impaired function or dysregulation of MAD2 is commonly associated with elevated rates of tumor cell proliferation, metastasis, and disease recurrence[18]. While the body of evidence concerning the involvement of SGO2 and MAD2 in various forms of malignancy continues to expand, the precise contributions of these proteins to the development and progression of LUAD remain relatively uncharted territories. Thus, it is of paramount importance to conduct thorough investigations aimed at elucidating the mechanisms through which SGO2 and MAD2 affect LUAD pathogenesis. Such research could provide critical insights into potential therapeutic targets and improve our understanding of LUAD biology. The present investigation was designed to delve into the significance of SGO2 in the context of LUAD and to examine its connection with MAD2. This was achieved through an integrative approach that included bioinformatics assessment and experimental verification. The insights gained from this research enrich our comprehension of SGO2's role in LUAD and highlight its promise as a potential prognostic indicator. Further investigation into the regulatory relationship between SGO2 and MAD2 may reveal new opportunities for advancing targeted therapies in LUAD.

Results

SGO2 is highly expressed in LUAD and other malignancies compared to normal tissues

An extensive pan-cancer study utilizing the TCGA dataset demonstrated elevated expression of SGO2 across various malignancies, encompassing bladder urothelial carcinoma (BLCA), breast invasive carcinoma (BRCA), cervical squamous cell carcinoma and endocervical adenocarcinoma (CESC), cholangiocarcinoma (CHOL), colon adenocarcinoma (COAD), esophageal carcinoma (ESCA), glioblastoma multiforme (GBM), head and neck squamous cell carcinoma (HNSC), kidney renal clear cell carcinoma (KIRC), liver hepatocellular carcinoma (LIHC), lung adenocarcinoma (LUAD), lung squamous cell carcinoma (LUSC), prostate adenocarcinoma (PRAD), rectum adenocarcinoma (READ), stomach adenocarcinoma (STAD), and uterine corpus endometrial carcinoma (UCEC). Contrarily, in specific cancer types such as KICH and THCA, a reduction in SGO2 expression was observed (Fig. 1A). Furthermore, we investigated the SGO2 expression patterns across different cancers using the GEPIA database (Fig. 1B). Seeking to understand the correlation between SGO2 expression and LUAD more thoroughly, we concentrated our analysis on the TCGA dataset. The findings revealed a notable upregulation of SGO2 in LUAD tissues compared to normal lung tissue ($p < 0.001$) (Fig. 2A). Moreover, SGO2 expression in LUAD tissues was notably higher than in adjacent non-cancerous tissues ($p < 0.001$) (Fig. 2B). We further analyzed SGO2 protein levels in the collected samples through immunohistochemical staining. Analysis of the data showed a significant increase in the expression of the SGO2 protein in LUAD tissues when contrasted with the surrounding benign lung tissue (Fig.2C). Additionally, we investigated the association between SGO2 expression levels and both the TNM and pathological stages of the disease, referring to the AJCC Cancer Staging Manual (8th ed.)[19]. Notably, SGO2 expression was higher in the later stages of T stages (T2-T4 vs. T1, $p < 0.001$), N stages (N1-N3 vs. N0, $p < 0.001$), and overall pathological stages (II-IV vs. I, $p < 0.001$; Fig. 2D). It appeared that the upregulation of SGO2 was significantly related to the worsening of LUAD.

High expression of SGO2 is associated with poor prognosis in LUAD patients

We aimed to determine the potential of SGO2 as a groundbreaking prognostic indicator for LUAD by employing the TCGA dataset to build Kaplan-Meier (K-M) survival plots and to gauge the effect of SGO2 expression levels on the forecasted outcomes for LUAD sufferers.Analysis of the data demonstrated a significant link between elevated SGO2 expression and a less favorable prognosis in individuals with LUAD. In detail, increased levels of SGO2 expression were significantly associated with shorter overall survival (OS) (HR = 1.64 [1.22-2.19], $p < 0.001$), shorter disease-specific survival (DSS) (HR = 1.97 [1.35-2.87], $p < 0.001$), and shorter progression-free survival (PFS) (HR = 1.47 [1.12-1.91], $p = 0.005$) (Fig.3A-C).In order to further substantiate the link between increased SGO2 expression and a worse prognosis in individuals with LUAD, we conducted survival analysis using the Prognoscan website, based on GEO database datasets GSE13213 and GSE31210. The analysis confirmed that high SGO2 expression was significantly correlated with poor overall survival in both datasets (HR = 1.62 [1.24-2.12], $p < 0.001$; HR = 2.22 [1.25-3.92], $p = 0.006$) (Fig.3D-E).Moreover, the receiver operating characteristic (ROC) curve analysis demonstrated that SGO2 had considerable diagnostic value for LUAD, scoring an area under the curve (AUC) of 0.873 (Fig.4A). These results pointed to a significant association between high SGO2 expression and unfavorable prognosis in LUAD patients, highlighting its potential as a promising prognostic indicator.

Knockdown of SGO2 markedly curtails proliferation, migration, and invasion in LUAD cells

Evaluating the SGO2 expression profiles in three LUAD cell lines (H1299, H1975, and A549) alongside the normal human lung epithelial cell line Beas-2B, our concurrent use of RT-qPCR and Western blot techniques revealed distinct differences in SGO2 expression levels. Specifically, the SGO2 mRNA and protein levels in normal Beas-2B cells served as a baseline control. Among LUAD cell lines, H1299 cells exhibited the highest SGO2 expression, with significantly elevated mRNA ($p < 0.0001$) and protein levels ($p < 0.01$) compared to Beas-2B cells. Notably, H1975 cells showed SGO2 expression levels comparable to those of Beas-2B cells ($p > 0.05$),

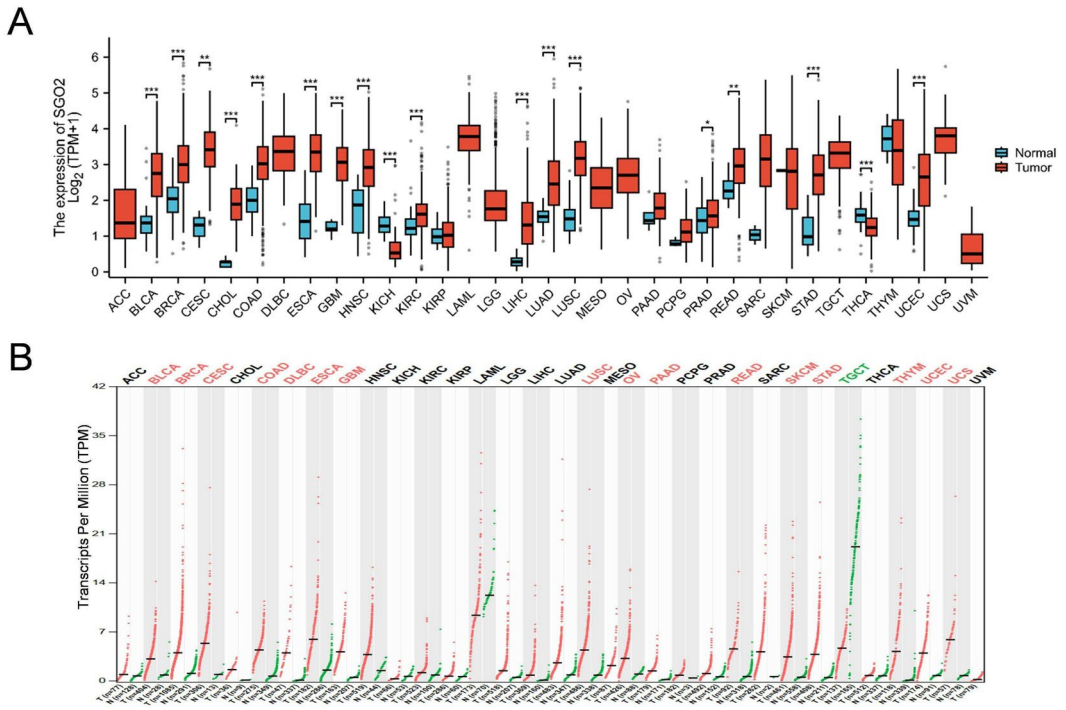

Fig. 1. Pan-Cancer Analysis of SGO2 Expression (**A**) SGO2 expression profiles across pan-cancers were analyzed using data from the TCGA database. Tumor samples (represented as red boxes) were compared against normal samples (represented as blue boxes) via the Mann-Whitney U test to assess expression differences. (**B**) SGO2 expression patterns across pan-cancers were interrogated utilizing the GEPIA web platform. Tumor samples (depicted as red dots) were contrasted with normal samples (depicted as green dots), with statistical testing following GEPIA's default analytical pipeline (*p < 0.05, **p < 0.01,***p < 0.001).

while A549 cells displayed the lowest SGO2 expression, even significantly lower than normal Beas-2B cells ($p < 0.01$) (Fig.5A-C). To further explore the functional significance of SGO2 in LUAD cells, we selected H1299 cells for subsequent experiments. Given that H1299 cells showed the highest SGO2 expression among LUAD cell lines and might be more sensitive to SGO2 knockdown due to their biological behaviors such as proliferation and invasiveness, this choice could more effectively demonstrate the impact of SGO2 depletion on LUAD cells.

Four siRNAs (si-SGO2-1051, si-SGO2-1609, si-SGO2-1768, and si-SGO2-3532) targeting SGO2 were designed and transfected into H1299 cells, with si-NC as a control to rule out non-specific interference effects. Both RT-qPCR ($p < 0.0001$) and Western blot ($p < 0.05$) results showed that si-SGO2-3532 significantly reduced SGO2 mRNA and protein expression (Fig.6A-B and Fig. S1). Therefore, si-SGO2-3532 was selected for subsequent phenotypic experiments. Initially, cell proliferation was assessed using the CCK-8 assay. The results demonstrated a significant decrease in H1299 cell proliferation after SGO2 knockdown ($p < 0.0001$) (Fig.6C). Furthermore, we conducted wound-healing and Transwell assays to gauge the influence of SGO2 on the migratory and invasive capabilities of H1299 cells. The findings indicated that cells treated with si-SGO2 exhibited significantly reduced migration ($p < 0.01$) and invasion ($p < 0.001$) compared to the si-NC control group (Fig.6D-E).The data from our experiments implied that SGO2 is integral to the processes of proliferation, migration, and invasion in H1299 cells, and reducing its expression markedly curtails these cellular behaviors.

SGO2 plays a crucial role in the EMT process

Epithelial-mesenchymal transition (EMT) is essential in the development, metastasis, and invasion stages of malignant tumors. We probed the function of SGO2 in EMT by knocking down its expression with si-SGO2-3532 and observed the effects on EMT-associated markers. The study revealed that the inhibition of SGO2 significantly decreased the expression of N-cadherin ($p < 0.05$) and Vimentin ($p < 0.05$), with no effect on the expression of E-cadherin ($p > 0.05$) relative to the control group (Fig. 6F).These findings suggested that SGO2 knockdown may suppress the EMT process by downregulating N-cadherin and Vimentin, thereby reversing the mesenchymal phenotype. At the same time, the stable expression of E-cadherin indicated that the epithelial phenotype is maintained. These results implied that SGO2 may promote the mesenchymal characteristics during EMT, thereby enhancing the migration and invasion capacity of tumor cells.

Knockdown of SGO2 disrupts cell cycle progression in LUAD cells

The above experiments demonstrated that SGO2 depletion inhibited LUAD cell proliferation. To explore whether SGO2 influenced cell proliferation through cell cycle regulation, by employing flow cytometry, we investigated how the knockdown of SGO2 affected the cell cycle. The analysis showed a substantial decline in the G1 phase

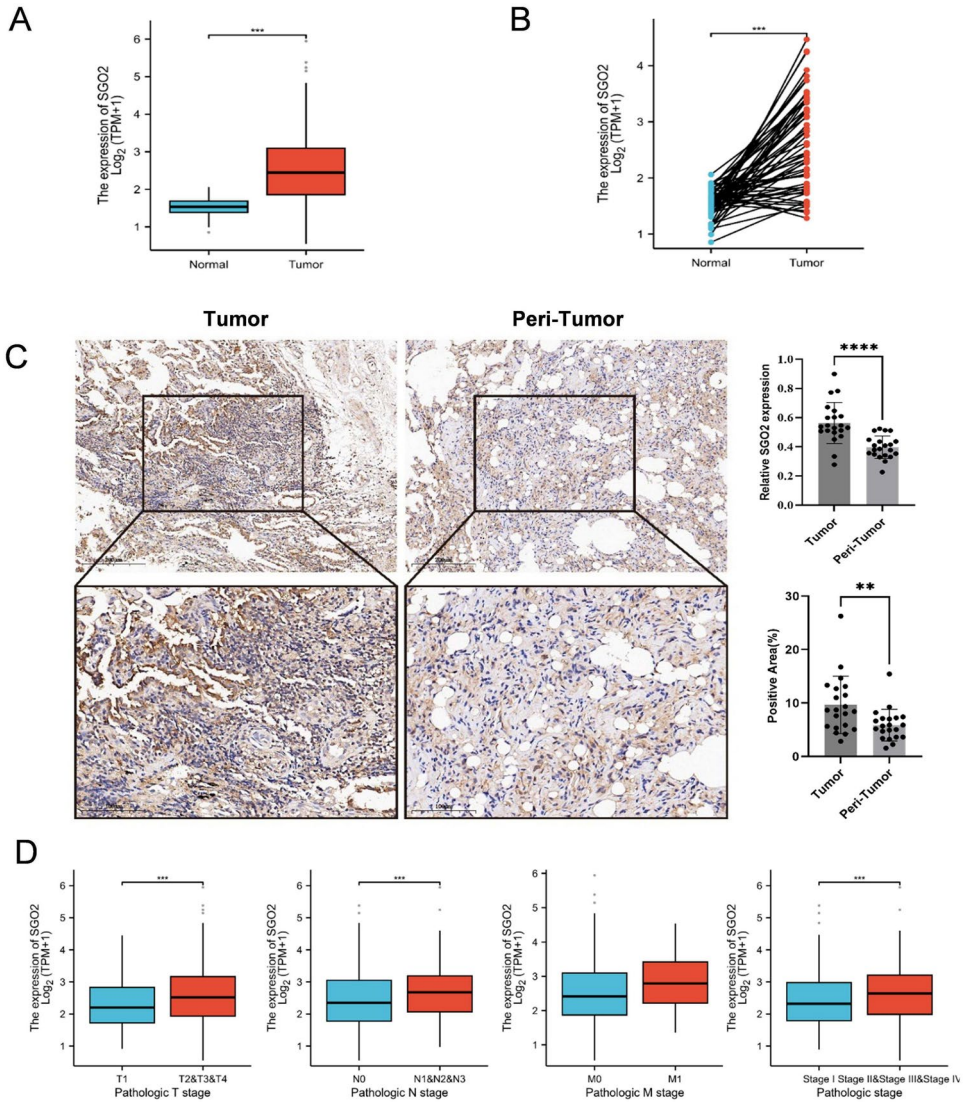

Fig. 2. Investigation of SGO2 Expression in LUAD. (**A**) Paired comparison: SGO2 expression in tumor vs. matched adjacent normal tissues from LUAD patients (paired t-test). (**B**) Unpaired comparison: SGO2 expression in tumor vs. normal tissues (unpaired t-test). (**C**) Immunohistochemical validation: Immunohistochemical analysis assessed SGO2 expression in LUAD tumor tissues and adjacent peri-tumor tissues from 21 patients (n = 21). Comparison of relative SGO2 expression levels (top) and positive staining area percentages (bottom) between tumor and peri-tumor tissues used paired t-test. (**D**) Clinical stage-related analysis: Based on the TCGA database, SGO2 expression was analyzed across subgroups of T stage, N stage, M stage, and pathological stage. Statistical method: One-way ANOVA with Bonferroni post-hoc test. (*$p < 0.05$, **$p < 0.01$, ***$p < 0.001$, ****$p < 0.0001$).

cell population ($p < 0.0001$) and a considerable increase in the G2/M phase cell population ($p < 0.0001$) upon SGO2 knockdown. These observations implied that the downregulation of SGO2 could lead to an arrest in the G2/M phase of the cell cycle, potentially interfering with cellular division (Fig.7A). Additionally, we investigated the protein expression linked to the cell cycle. The cells with SGO2 knockdown displayed significantly reduced expression of Cyclin D1 (G1 phase marker; $p < 0.05$) and increased expression of Cyclin B1 (G2/M phase marker; $p < 0.001$) when compared to the control group (Fig.7B). These data implied that SGO2 played a critical role in modulating the cell cycle and may inhibit cell division by disrupting cell cycle homeostasis.

SGO2-related differentially expressed genes (DEGs) have significant functions in cell division

To further explore the biological significance of SGO2-related differentially expressed genes (DEGs), Gene Ontology (GO) and Kyoto Encyclopedia of Genes and Genomes (KEGG) enrichment analyses were conducted (Fig.8A). The findings from the GO analysis indicated that DEGs were highly enriched in various biological processes(BP), especially those involved in mitotic nuclear division and organelle fission, implying that these genes have significant functions in the processes of cell cycle and cell division.Cellular component (CC) analysis further showed that DEGs were primarily located in the condensed chromosome, centromere region, and

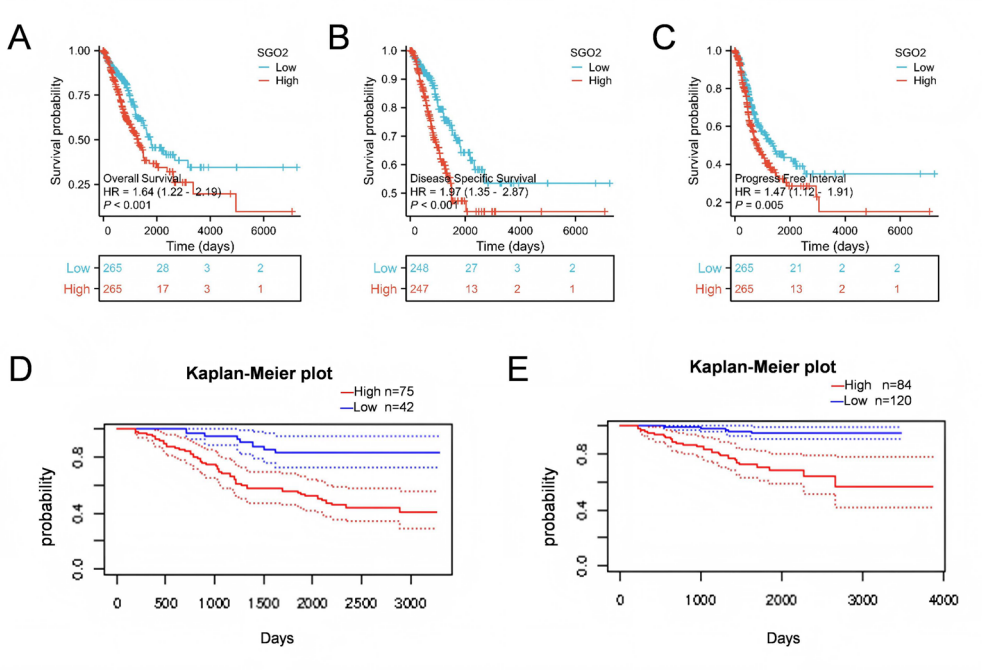

Fig. 3. Elevated SGO2 expression was associated with poor prognosis in LUAD patients. (**A**-**C**) Kaplan-Meier survival analyses (via log-rank test) from TCGA database comparing LUAD patients with high vs. low SGO2 expression (stratified by median). (**A**) OS: High-expression group (n = 265) showed significantly worse prognosis than low-expression group (n = 265) (HR = 1.64, p < 0.001). (**B**) DSS: High-expression group (n = 247) had poorer outcomes than low-expression group (n = 248) (HR = 1.87, p < 0.001). (**C**) PFS: High-expression group (n = 265) exhibited shorter PFS than low-expression group (n = 265) (HR = 1.47, p = 0.005). (**D**-**E**) Validation in GEO datasets (log-rank test): (**D**) GSE13213: High-expression group (n = 75) had significantly reduced survival vs. low-expression group (n = 42) (p < 0.01). (**E**) GSE31210: High-expression group (n=84) showed worse prognosis compared to low-expression group (n = 120) (p = 0.005). HR: Hazard ratio.

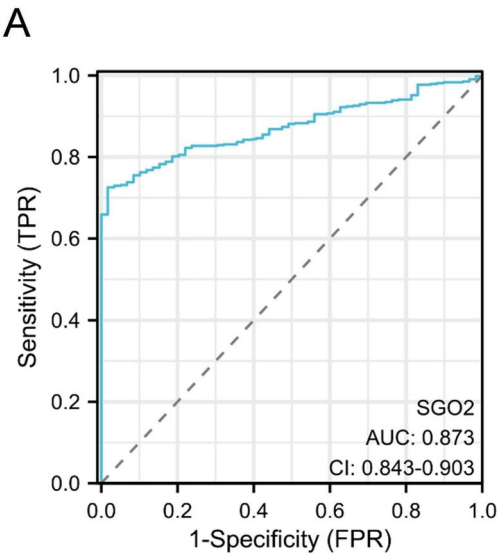

Fig. 4. The diagnostic ROC curve for SGO2. (**A**) Receiver operating characteristic (ROC) curve evaluating SGO2 expression as a diagnostic biomarker for LUAD. The area under the curve (AUC) was 0.873 (95% CI: 0.843-0.903), indicating high discriminatory power.

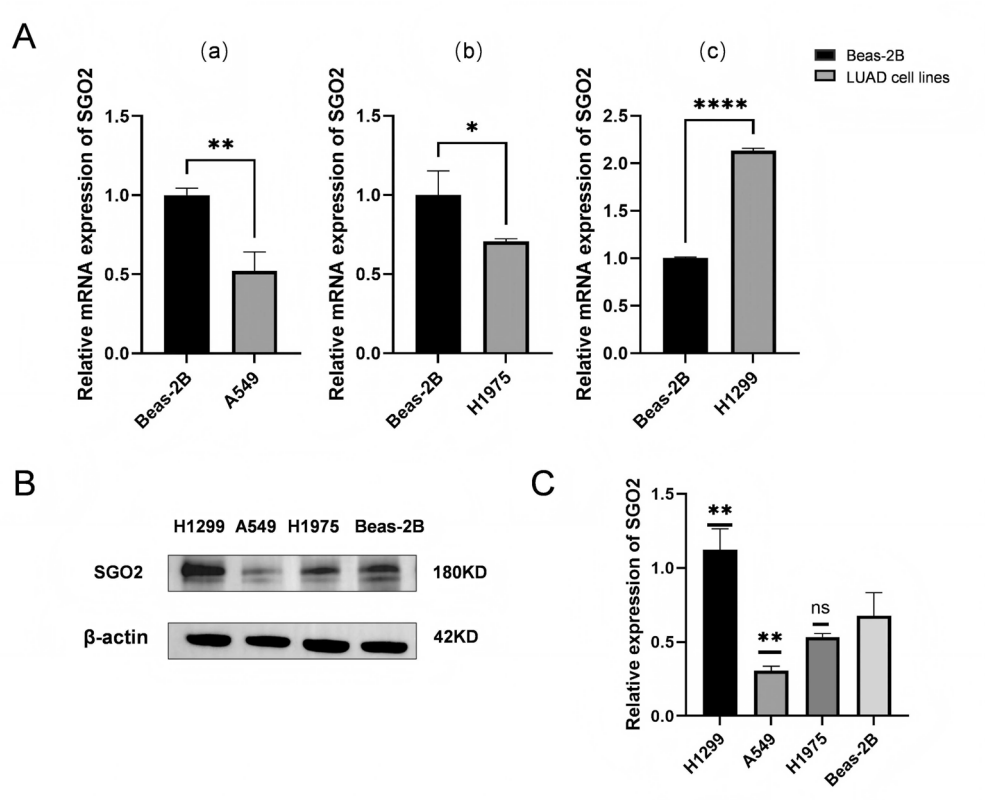

Fig. 5. SGO2 expression in LUAD cell lines relative to normal Beas-2B cells. (**A**) Combined subpanels showing relative SGO2 mRNA expression: (**a**-**c**) Relative SGO2 mRNA expression in A549 (**a**), H1975(**b**) and H1299 (**c**) cells, normalized to Beas-2B. (n = 3, Student's t-test). (**B**-**C**) Representative western blot (**B**) and quantitative analysis (**C**) of SGO2 protein expression in the same cell lines. β-actin served as the loading control (n = 3, one-way ANOVA with Tukey's post hoc test). Original blots are shown in Fig. S2. (*p < 0.05, **p < 0.01, ***p < 0.001, ****p < 0.0001).

chromosomal region, highlighting their critical functions in chromosome structure during cell division. Results from the Molecular Function (MF) analysis proposed that SGO2 is central to the mechanisms of chromosome segregation and protein hydrolysis. In addition, the analysis of KEGG pathways suggested that SGO2 could be implicated in several biological pathways, encompassing the immune response and the regulation of the cell cycle, thereby underlining the critical function of SGO2 in regulating cell division.

SGO2 mediates LUAD cell migration and invasion via MAD2

Given the possible interaction pathways involving SGO2 and MAD2, this research further explored their expression profiles and correlation in LUAD cellular models. Analysis of the data uncovered a significant positive association between SGO2 and MAD2 expression in LUAD cells ($p < 0.001$) (Fig.8B). To establish SGO2-overexpressing cell models, H1299 cells were transfected with the SGO2 overexpression plasmid pENTER-SGO2(human)-FLAG-6×His-Puro using jetPRIME transfection reagent, following the protocol described in the Materials and Methods section. Empty vector-transfected cells were used as controls. Results showed significantly elevated SGO2 protein ($p < 0.01$) and mRNA ($p < 0.05$) levels in cells transfected with the SGO2 overexpression plasmid compared to empty vector controls, confirming successful establishment of overexpression models (Fig.8C-D). Detailed investigation revealed that reducing SGO2 expression led to a significant decrease in MAD2 levels ($p < 0.05$), while an increase in SGO2 expression also caused higher MAD2 expression ($p < 0.01$) (Fig.8C). To investigate whether the influence of SGO2 on LUAD cell proliferation and migration is mediated through MAD2, we applied the MAD2-specific inhibitor M2I-1 to H1299 cells that had been engineered for SGO2 overexpression. SGO2-overexpressing cells were pre-treated with 10 μM M2I-1 for 24 hours before functional assays. Results showed that MAD2 inhibition substantially reduced the increased migration ($p < 0.001$) and invasion ($p < 0.01$) capabilities observed in SGO2-overexpressing cells (Fig.8E). These findings suggested that SGO2 might augment the migratory and invasive properties of LUAD cells via its regulation of MAD2 expression.

Discussion

The LUAD is a leading cause of cancer-related mortality worldwide, and its aggressive invasiveness and metastatic potential present significant challenges in treatment management. While targeted therapies have demonstrated

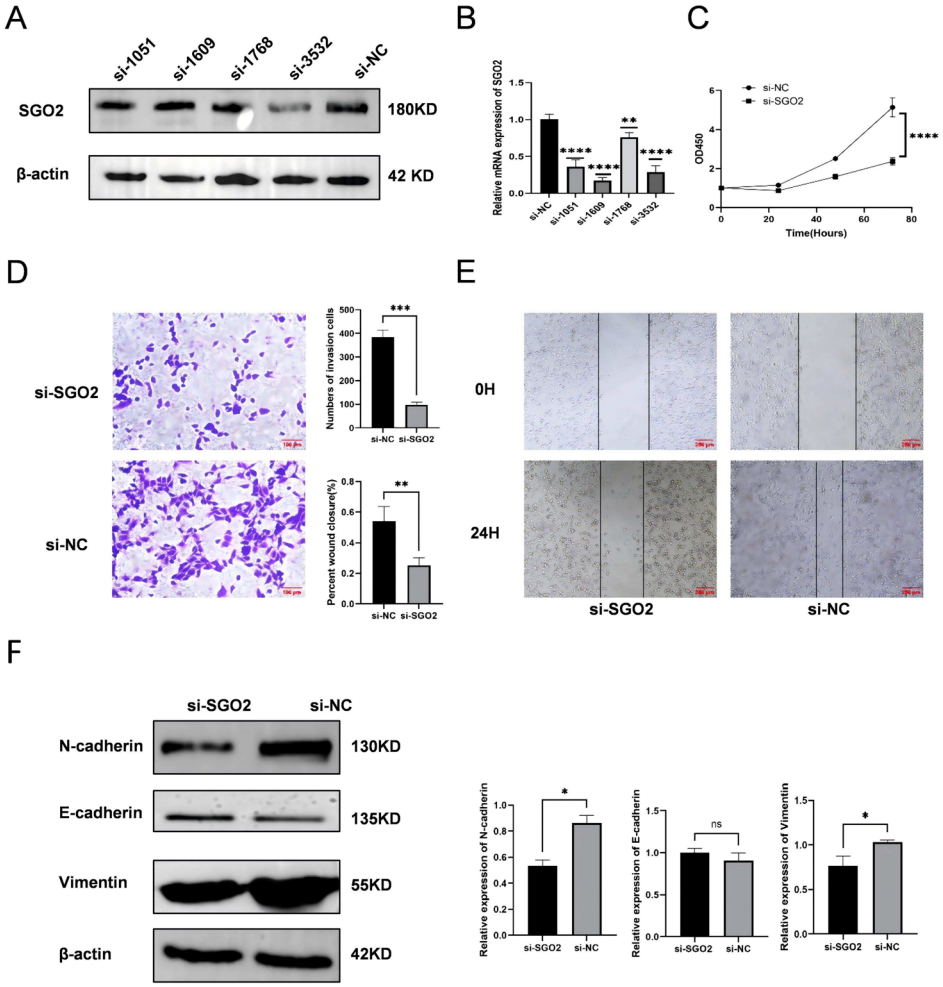

Fig. 6. SGO2 knockdown suppressed malignant behaviors in LUAD cells. (**A**-**B**) Validation of siRNA-mediated SGO2 knockdown efficiency by (**A**) qPCR and (**B**) Western blot. (n = 3, one-way ANOVA with Tukey's post hoc test). (**C**-**E**) Proliferation (CCK-8), migration (wound healing), and invasion (Matrigel) assays in SGO2-depleted H1299 cells. (n = 3, Student's t-test). (**F**) Western blot analysis of EMT markers (N-cadherin, E-cadherin, Vimentin) in SGO2-knockdown H1299 cells with β-actin served as loading control. (n = 3, Student's t-test). Original blots are shown in Fig. S3-6. (*p < 0.05, **p < 0.01, ***p < 0.001, ****p < 0.0001).

potential in extending survival in patients with advanced LUAD, the current treatments have limited coverage of molecular targets, resulting in certain limitations. Therefore, there is an urgent need to explore novel molecular targets and gain a comprehensive understanding of their mechanisms to improve the therapeutic efficacy for LUAD. Analyses of the TCGA and GEPIA repositories revealed that SGO2 expression was substantially elevated in LUAD, showing a relative enhancement in cancerous LUAD tissues over adjacent normal tissues. We further validated these findings by collecting LUAD patient samples for immunohistochemical analysis, which confirmed the elevated expression of SGO2 in LUAD tissues. Also, a strong association was noted between the expression of SGO2 and both TNM staging and pathological grading. This is in line with previous investigations that have revealed a high expression of SGO2 in multiple cancer types to be intricately connected to the progression of tumors, their metastatic potential, and a poor outlook for patients[20,21]. The current findings suggested a crucial role for SGO2 in the initiation and evolution of LUAD. To investigate the functional role of SGO2 in LUAD, we engineered a LUAD cell line with decreased SGO2 expression using siRNA technology. The attenuation of SGO2 significantly abrogated the proliferative, migratory, and invasive capacities of the LUAD cells. The combined utilization of the CCK-8 assay, wound healing assay, and Transwell assay corroborated the pivotal role of SGO2 in the biological attributes of LUAD cells.

The onset and progression of cancer are typically associated with increased genomic instability, with accurate chromosome segregation being essential for maintaining genome stability, and chromosomal instability is considered a key driver of cancer progression[22–24] As a member of the Shugoshin family, SGO2 is essential in the cell division process, particularly during meiosis and mitosis, by governing the precise segregation of chromosomes to uphold genomic stability[25–29]. The KEGG pathway analysis suggested that SGO2 could be implicated in several biological pathways, encompassing the immune response and the regulation of the cell cycle, thereby underlining the critical function of SGO2 in regulating cell division. Concurrently, the GO

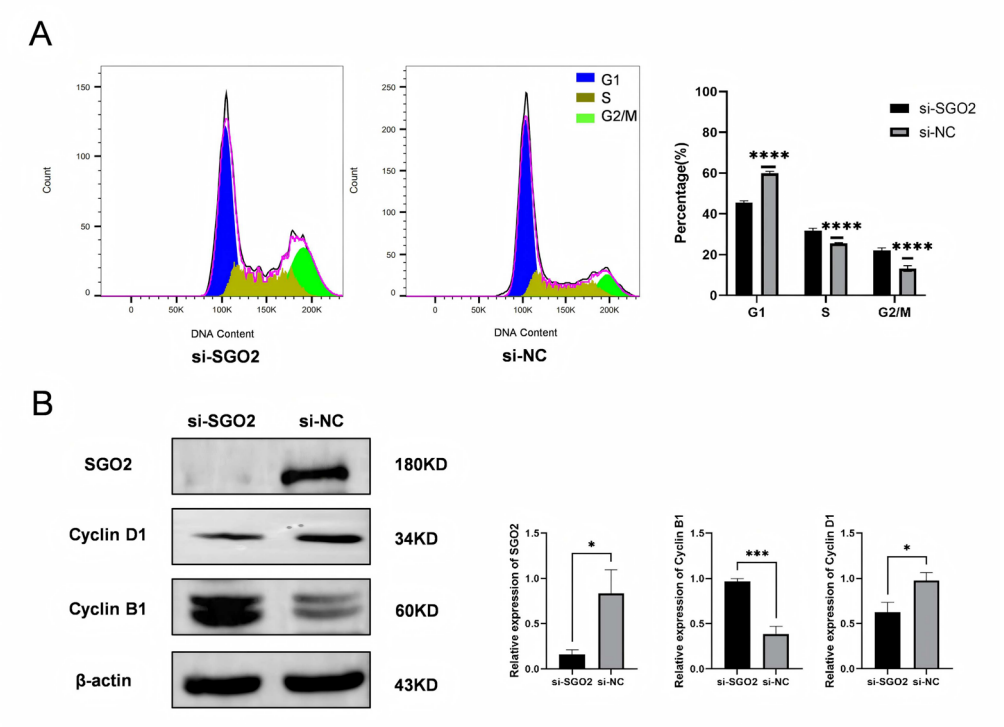

Fig. 7. Knockdown of SGO2 affected the cell cycle in LUAD cells. (**A**) Flow cytometry analysis of cell cycle distribution (G1, S, G2/M phases) in si-SGO2 and si-NC groups. (n = 3, two-way ANOVA with Sidak's test). (**B**) Western blot of cell cycle proteins (Cyclin B1, Cyclin D1). β-actin served as control (n = 3, Student's t-test). Original blots are shown in Fig. S7-9. (*p < 0.05, **p < 0.01, ***p < 0.001, ****p < 0.0001).

analysis results indicated that in DEGs, the genes involved in mitosis, mitosis and organelle fission were highly enriched in multiple biological processes (BP), which aligns with the KEGG findings. Results from the Molecular Function (MF) analysis proposed that SGO2 is central to the mechanisms of chromosome segregation and protein hydrolysis, further explaining its role in cellular processes. Cellular component (CC) analysis further showed that DEGs were primarily located in the condensed chromosome, centromere region, and chromosomal region, highlighting their critical functions in chromosome structure during cell division. Among them, a possible target MAD2 related to SGO2 plays a pivotal role in spindle assembly checkpoint. The functions of SGO2 and MAD2 in cell division are intricately linked, especially during mitosis[30]. SGO2, as a pivotal player in chromosome segregation, primarily ensures accurate chromosome distribution during cell division by preserving the cohesion of sister chromatids[31]. MAD2, as a crucial component of the spindle assembly checkpoint protein complex, predominantly functions to monitor the correct alignment of chromosomes at the metaphase plate during early mitosis, thereby preventing erroneous chromosome segregation[32]. During the cell cycle, the dysregulation of SGO2 and MAD2 may lead to chromosomal instability and contribute to the occurrence of various types of cancer. We attempted to clarify the role of SGO2 in the cell cycle and its association with MAD2 in LUAD in order to evaluate its potential participation in tumor progression.

A notable finding from our research was the influence of SGO2 on cell cycle progression. The depletion of SGO2 effectively arrested the transition from G1 to S phase and increased the proportion of cells in the G2/M phase. Furthermore, Cyclin D1 was significantly downregulated while Cyclin B1 was significantly upregulated in SGO2-knockdown cells. These data indicate that SGO2 plays a key role in regulating the cell cycle and may potentially inhibit cell division by disrupting cell cycle homeostasis.

SGO2 and MAD2 exhibit a significant positive correlation in LUAD cells. Following the depletion of SGO2, the expression level of MAD2 markedly diminished, while the overexpression of SGO2 resulted in a significant elevation in MAD2 expression. Subsequent experimentation disclosed that the attenuation of MAD2 could revert the enhanced migratory and invasive capacities induced by SGO2 overexpression. SGO2 was proposed to regulate MAD2 expression and participate in cellular division, thereby promoting the migration and invasion of LUAD cells. These findings provided a novel perspective on the role of SGO2 in LUAD and suggest potential directions for exploring targeted therapeutic strategies that focus on the SGO2-MAD2 axis. However, the specific regulatory mechanism by which SGO2 affects the expression of MAD2 remains unclear, and more experiments are needed to further determine it. Additionally, the experimental design of this part of the study has certain imperfections that need to be further explored in follow-up research. Specifically, future studies could employ A549 cells (with lower basal SGO2 expression than H1299 cells) to overexpress SGO2, thereby circumventing potential baseline interference from high endogenous SGO2 levels in H1299 cells. This approach would help validate whether the SGO2-MAD2 axis exerts conserved regulatory effects on cell migration and

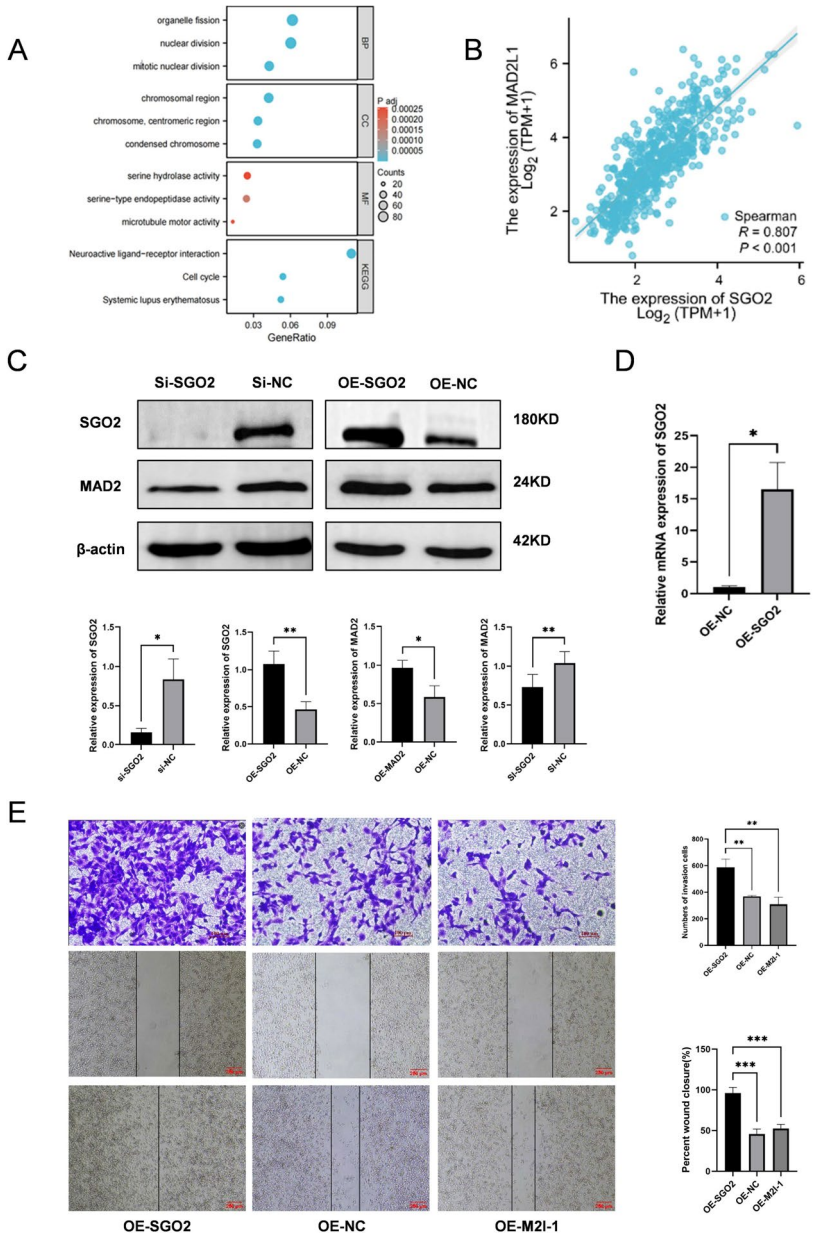

Fig. 8. SGO2 regulated LUAD cell migration and invasion via MAD2. (**A**) GO and KEGG enrichment analysis of genes associated with SGO2. (The use permission from Kanehisa Laboratories has been obtained.) (**B**) Correlation analysis between SGO2 and MAD2 expression (Pearson's R = 0.62, p < 0.001). (**C-D**) Verification of SGO2 overexpression efficiency using qPCR and Western blot, and analysis of MAD2 expression following SGO2 knockdown or overexpression (n = 3, Student's t-test). (**E**) Invasion and migration assays of H1299 cells in three groups: SGO2 overexpression (OE-SGO2), control (OE-SGO2-NC), and SGO2-OE with MAD2 inhibitor (OE-M2I-1) (n = 3, one-way ANOVA with Tukey's post hoc test). Original blots are shown in Fig. S10-12. (*p < 0.05, **p < 0.01, ***p < 0.001, ****p < 0.0001).

invasion across LUAD cell lines with distinct SGO2 expression profiles. Additionally, investigating whether MAD2 overexpression rescues the phenotypic changes caused by SGO2 knockdown would further clarify the functional dependency of SGO2 on MAD2 in LUAD progression.

Furthermore, the EMT is crucial for tumor development and invasion; upon SGO2 knockdown, there was a significant reduction in the expression levels of EMT markers, such as N-cadherin and Vimentin. This suggests that SGO2 may promote the acquisition of mesenchymal characteristics in LUAD cells by modulating the EMT pathway, thereby enhancing the migratory and invasive potential of cancer cells.

According to our current research and relevant literature, SGO2 primarily regulates chromosomal stability through its interaction with MAD2[17], and it may induce chromosomal instability to indirectly affect the EMT process. Although studies have shown that EMT can induce chromosomal instability[33,34], this study found that SGO2 downregulation led to reduced expression of EMT markers (such as N-cadherin and vimentin), suggesting

that EMT is inhibited. We speculate that this effect is more likely a byproduct of SGO2's direct regulation of chromosome segregation (such as cell cycle arrest) rather than being mediated by classical EMT transcription factors (such as Twist and ZEB1). It is important to note that this study did not detect the protein levels of Twist and ZEB1, and their potential roles still need further verification. The existing data indicate that the regulation of chromosomal stability by the SGO2-MAD2 interaction may function independently of the classical EMT pathway, but it does not exclude the possibility of cross-regulation between the two in specific microenvironments or tumor progression stages. Future research is required to further clarify the precise molecular connections between CIN and EMT, particularly whether and how the SGO2-MAD2 complex specifically regulates key EMT transcription factors.

Although this study has clarified the critical role of SGO2 in LUAD and its association with MAD2, several limitations should be acknowledged. First, while we characterized SGO2 functions in cell proliferation, migration, invasion, and other biological processes using the H1299 cell line, the exclusive reliance on a single cell line may limit the generalizability of our findings. Second, although in vitro experiments have provided mechanistic insights, in vivo validation using LUAD animal models is essential to confirm the physiological relevance of SGO2-MAD2 axis. Additionally, the interaction between SGO2 and other cell cycle regulators remains unexplored, which is critical for comprehensively elucidating SGO2-mediated tumorigenic pathways in LUAD.

Summary

The results of this study reveal that SGO2 is overexpressed in LUAD and is significantly associated with a poorer prognosis in patients. The participation of SGO2 in regulating a diverse array of biological processes, including cell proliferation, migration, invasion, and cell cycle regulation, implies a pivotal role in the onset and progression of LUAD. We also found that the regulatory effect of SGO2 on MAD2 may be a key mechanism by which it promotes tumor cell migration and invasion. Therefore, targeted therapeutic strategies based on the interaction between SGO2 and MAD2 may offer new insights for the treatment of LUAD.

Methods

Clinical samples

This study included clinical and pathological samples from 21 patients who underwent surgical resection at Nanjing Second Hospital between March and June 2024. The samples comprised both lung adenocarcinoma tissues and adjacent non-cancerous tissues. Authorization for this research was provided by the Ethics Committee at Nanjing Second Hospital (Approval No. 2024-LS-ky-013).

SGO2 expression analysis

The mRNA expression levels of SGO2 were systematically analyzed using data from The Cancer Genome Atlas (TCGA) database (https://portal.gdc.cancer.gov) and the GEPIA2 online platform (http://gepia2.cancer-pku.cn/). RNA-seq data (STAR pipeline, TPM format) from 33 tumor types were downloaded from TCGA and processed using R (Version 4.2.1, https://cran.r-project.org/). Statistical analyses were performed using the "stats" package (Version 4.2.1, https://cran.r-project.org/) and "car" package (Version 3.1.0, https://cran.r-project.org/package=car), with appropriate statistical methods selected based on data distribution characteristics. If data failed to meet statistical assumptions (e.g., normality or homogeneity of variance), analyses were either terminated or non-parametric methods were employed. For differential expression analysis of SGO2 between clinical subgroups, Mann-Whitney U tests were performed using R (Version 4.2.1, https://cran.r-project.org/), with statistical significance set at $p < 0.05$. All data visualizations were generated using the "ggplot2" package (Version 3.4.4, https://cran.r-project.org/package=ggplot2).

Prognostic analysis, diagnostic analysis, and functional enrichment analysis

To obtain clinical follow-up data of LUAD patients and extract SGO2 mRNA expression profiles, we accessed the TCGA database. Using the "survival" package (Version 3.3.1, https://cran.r-project.org/package=survival) in R, proportional hazards assumption tests were performed to validate the Cox model, enabling subsequent survival regression analysis. Visualization of results was conducted using "survminer" (Version 3.4.4, https://cran.r-project.org/package=survminer) and "ggplot2" (Version 3.4.4, https://cran.r-project.org/package=ggplot2). Specifically, Kaplan-Meier curves were plotted to show survival probability over time, with log-rank tests used to assess intergroup differences. Hazard ratios (HR), 95% confidence intervals (CI), and p values were annotated in the figures. External validation of prognostic analyses was performed using an independent dataset from PrognoScan (http://dna00.bio.kyutech.ac.jp/PrognoScan/). For diagnostic efficacy evaluation, ROC curve analysis was conducted via the "pROC" package (Version 1.18.0, https://cran.r-project.org/package=pROC) to calculate AUC, with results visualized using "ggplot2" (Version 3.4.4, https://cran.r-project.org/package=ggplot2). Utilizing the clusterProfiler package (Version 4.8.3, https://bioconductor.org/packages/clusterProfiler), we performed enrichment analyses for Gene Ontology (GO) and Kyoto Encyclopedia of Genes and Genomes (KEGG) pathways to investigate the functional implications of genes differentially expressed in relation to SGO2 (Padj < 0.05, $|\mathrm{LogFC}| \geq 1$). The results of these analyses were subsequently visualized utilizing the ggplot2 package (Version 3.4.4, https://cran.r-project.org/package=ggplot2) for graphical depiction.

Correlation analysis

Spearman's rank correlation coefficient was used to analyze the relationship between SGO2 and MAD2. Briefly, mRNA or protein expression data of SGO2 and MAD2 were extracted from experimental and control groups, ensuring the data distribution met the requirements for non-parametric testing. The cor.test() ("stats"

siRNA	Sense	Anti-sense
si-SGO2-1051	GUCUGCCAGAGAACCUAAUTT	AUUAGGUUCUCUGGCAGACTT
si-SGO2-1609	GUCUGCCAGAGAACCUAAUTT	AGUUAGGGAAUUCUGACCCTT
si-SGO2-1768	CACCAAAGAUAAUGGAAAUTT	AUUUCCAUUAUCUUUGGUGTT
si-SGO2-3532	GAGCGUUUCUUCUGGUAAATT	UUUACCAGAAGAAACGCUCTT
si-NC	UUCUCCGAACGUGUCxACGUTT	ACGUGACACGUUCGGAGAATT

Table 1. The siRNAs constructed in this study.

Name	Dilution ratio	Catalog number	Brand
SGO2 antibody	1:1000	A08632	Boster
MAD2 antibody	1:1000	66014-1-Ig	Proteintech
N-Cadherin antibody	1:2000	22018-1-AP	Proteintech
E-Cadherin antibody	1:20000	20874-1-AP	Proteintech
Vimentin antibody	1:20000	60330-1-Ig	Proteintech
Cyclin D1 antibody	1:5000	60186-1-Ig	Proteintech
Cyclin B1 antibody	1:2000	55004-1-AP	Proteintech
β-actin antibody	1:10000	AC026	Abclone

Table 2. The primary antibodies used in this study.

package, Version 4.2.1, https://cran.r-project.org/) function in R (Version 4.2.1, https://cran.r-project.org/) was employed to compute the Spearman correlation coefficient (R value) and assess its statistical significance ($p < 0.05$ indicating significant correlation). To visually depict the correlation, scatter plots were generated using the "ggplot2" package (Version 3.4.4, https://cran.r-project.org/package=ggplot2), with SGO2 expression on the x-axis and MAD2 expression on the y-axis. Each plot included a fitted curve, along with annotations of the correlation coefficient (R value) and significance level (p value).

Cell culture and transfection

Cell lines A549, H1299, and H1975, which are derived from lung adenocarcinoma, along with normal lung epithelial cells Beas-2B, were acquired from Procell (Wuhan). These cells were maintained in 1640 medium (KGL 1501-500, KeyGEN BioTECH, Nanjing) enriched with 10% fetal bovine serum (NCS-500, newzerum, New Zealand) and 1% penicillin-streptomycin, and incubated at 37°C under a 5% CO2 atmosphere. At a cell density ranging from 30% to 50%, transfection was performed using anti-siRNA (GenePharma, Suzhou) (Table 1) and RFect V2 transfection reagent (11042, Baidai Biotechnology, Changzhou). The SGO2 overexpression plasmid pENTER-SGO2(human)-FLAG-6×His-Puro was purchased from Miaoling Biology (Wuhan). Upon achieving a cell density of roughly 60%, a mixture consisting of 2 μg of plasmid DNA and 200 μL of jetPRIME Buffer was vigorously vortexed for a duration of 10 seconds. Subsequently, 4 μL of the jetPRIME reagent was introduced into the blend, which was then allowed to incubate at ambient temperature for a 10-minute period. This prepared transfection mixture was subsequently transferred into a 6-well plate. Following a 4-hour interval, the existing medium was discarded and replaced with a complete culture medium. The cells were then cultured for an extended period of 48 hours before moving on to the next experimental steps.

Western blotting

The cell lysis was performed on ice for a duration of 10 minutes using RIPA buffer (R0010, Solarbio, Beijing). After lysis, the samples were subjected to centrifugation at 12,000 rpm for 10 minutes to separate the supernatant. The protein concentration was quantified utilizing a BCA protein assay kit (P0010, Beyotime, Shanghai). Protein samples, ranging from 20-30 μg, were then applied to a SDS-PAGE gel for electrophoresis. Following electrophoresis, the proteins were electrotransferred onto a PVDF membrane, which was subsequently blocked at room temperature with a 5% solution of non-fat dry milk for 1.5 hours. The membrane was then probed overnight at 4°C with the primary antibody, followed by a 1-hour incubation at room temperature the next day with the secondary antibody. The protein bands were visualized using an enhanced chemiluminescence (ECL) detection kit (Proteinbio Biotech, Nanjing).The antibodies used are listed in Table 2.

Real-time quantitative PCR (qRT-PCR)

For qRT-PCR, primers were purchased from Invitrogen (Shanghai, China) (Table 3). RNA extraction was conducted with the FastPure Cell/Tissue Total RNA Isolation Kit V2 (Vazyme Biotech, Nanjing). For the synthesis of cDNA, the HiScript III All-in-one RT SuperMix Perfect for qPCR (Vazyme Biotech, Nanjing) was used. The quantitative real-time PCR (qRT-PCR) assays were executed on a real-time PCR system, employing the Taq Pro Universal SYBR qPCR Master Mix supplied by Vazyme Biotech (Nanjing). The 2^-ΔΔ CT approach was employed to assess the relative gene expression levels, utilizing 18S rRNA as a reference gene.

Primer	Forward	Reverse
SGO2	5'-GTGATGGAGTGCCCAGTGAT -3'	5'-GCTAATGCCCTGTTGTTGTG-3'
18S rRNA	5'-GGAGTATGGTTGCAAAGCTGA-3'	5'-ATCTGTCAATCCTGTCCGTGT-3'

Table 3. The primers constructed in this study.

Cell proliferation assay
A density of 3,000 cells per well was adopted for culturing cells in 96-well plates. After achieving attachment, the cells were transfected with siRNA. Monitoring cell growth at 0, 24, 48, and 72 hours involved the CCK-8 assay (C0038, Beyotime, Shanghai), where absorbance was captured at 450 nm.

Scratch assay
A 6-well plate was used for seeding the cells, which were then transfected as previously outlined. Subsequent to the transfection process, the cells were incubated until they covered roughly 80% of the well surface. A distinct, linear injury was created with the aid of a 200 μL pipette tip, with care taken to maintain the correct width and consistency. The medium supplemented with 10% FBS was switched out for one with 2% FBS. Snapshots were taken at the 0-hour and 24-hour intervals with a microscope (Nikon, Japan).

Invasion assay
Cells that had been transfected were collected through a process of digestion followed by centrifugal separation, after which they were reconstituted in a serum-free culture medium. The concentration of cells was diluted to 2×10^5 cells/ml. The bottom compartment of the transwell apparatus was then loaded with a medium supplemented with 10% FBS, and the transwell insert was inserted into a 12-well plate. An amount of 100 μL of the prepared cell suspension was introduced into the upper compartment of the transwell system. Following an incubation period of 24 hours, the insert was taken out, immobilized in 4% paraformaldehyde solution for a half-hour, and then subjected to a 15-minute staining process with 0.1% crystal violet solution. Subsequently, the cells adhering to the lower surface of the insert were captured in images using a microscope from Nikon (Japan).

Cell cycle analysis
A population of 1×10^6 transfected cells was harvested and subjected to a single wash with chilled PBS, followed by centrifugation to remove the supernatant. The resulting cell pellet was then reconstituted in 2 mL of cool 75% ethanol, thoroughly mixed, and stored at 4°C for overnight fixation. The following day, a staining solution consisting of Propidium Iodide (PI) and RNase A in a 1:9 volume ratio (KGA9101-100, KeyGEN BioTECH, Nanjing) was prepared, and 500 μL of this mixture was employed for cell staining. Subsequently, the stained cells were analyzed using flow cytometry on a BD FACSCanto II instrument, with the obtained data being analyzed using FlowJo software (Version 10.8.1).

Immunohistochemistry
Tissues were first fixed, sectioned, and deparaffinized, followed by antigen retrieval through heating. Non-specific binding was blocked using a blocking solution. The tissue sections were treated with a primary antibody specific to SGO2 (dilution 1:50, catalog number 30867-1-AP, Proteintech, Wuhan), and subsequently, a secondary antibody linked to an enzyme was applied. Subsequent to this, a chromogenic reagent was introduced to enable the detection of the target protein, while the cell nuclei were stained with hematoxylin as a contrast. The dehydration, clearing, and mounting procedures were then carried out on the sections. The stained sections were subsequently examined using a microscope to observe the results.

Data analysis
Analysis of the data was conducted with GraphPad Prism version 9.0.1, and the results are expressed as the average plus or minus the standard deviation (SD). Comparisons between groups were assessed through unpaired t-tests or one-way ANOVA. A p-value of less than 0.05 was deemed to indicate statistical significance. * $p < 0.05$,** $p < 0.01$,*** $p < 0.001$,**** $p < 0.0001$. Each experimental procedure was independently replicated three times.

Data availibility
The corresponding author will provide the raw data supporting the conclusions of this article, with no undue restrictions.

Received: 5 April 2025; Accepted: 7 July 2025
Published online: 15 July 2025

References
1. Lee, Y. S., Yeo, I. J., Kim, K. C., Han, S.-B. & Hong, J. T. Inhibition of lung tumor development in apoe knockout mice via enhancement of trem-1 dependent nk cell cytotoxicity. *Front. Immunol.* **10**, 1379 (2019).
2. Thai, A., Solomon, B., Sequist, L., Gainor, J. & Heist, R. *Lung cancer. lancet lond engl* **398**, 535–554 (2021).
3. Bray, F. et al. Global cancer statistics 2022: Globocan estimates of incidence and mortality worldwide for 36 cancers in 185 countries. *CA: a cancer journal for clinicians* **74**, 229–263 (2024).

4. Kadara, H. et al. Whole-exome sequencing and immune profiling of early-stage lung adenocarcinoma with fully annotated clinical follow-up. *Ann. Oncol.* **28**, 75–82 (2017).
5. Zhang, M. et al. An immune-related signature predicts survival in patients with lung adenocarcinoma. *Front. Oncol.* **9**, 1314 (2019).
6. Goldstraw, P. et al. Non-small-cell lung cancer. *The Lancet* **378**, 1727–1740 (2011).
7. Tseng, C.-H. et al. The relationship between air pollution and lung cancer in nonsmokers in taiwan. *J. Thorac. Oncol.* **14**, 784–792 (2019).
8. Kim, H. C. et al. Five-year overall survival and prognostic factors in patients with lung cancer: results from the korean association of lung cancer registry (kalc-r) 2015. *Cancer Research and Treatment: Official Journal of Korean Cancer Association* **55**, 103–111 (2022).
9. Carnio, S., Novello, S., Mele, T., Levra, M. G. & Scagliotti, G. V. Extending survival of stage iv non-small cell lung cancer. *Semin. Oncol.* **41**, 69–92 (2014).
10. Kitajima, T. S. et al. Shugoshin collaborates with protein phosphatase 2a to protect cohesin. *Nature* **441**, 46–52 (2006).
11. Yan, K. et al. Structure of the inner kinetochore ccan complex assembled onto a centromeric nucleosome. *Nature* **574**, 278–282 (2019).
12. Deng, M. et al. High sgo2 expression predicts poor overall survival: a potential therapeutic target for hepatocellular carcinoma. *Genes* **12**, 876 (2021).
13. Hu, Q., Liu, Q., Zhao, Y., Zhang, L. & Li, L. Sgol2 is a novel prognostic marker and fosters disease progression via a mad2-mediated pathway in hepatocellular carcinoma. *Biomark. Res.* **10**, 82 (2022).
14. Lv, T. et al. Sgol2 promotes prostate cancer progression by inhibiting rab1a ubiquitination. *Aging (Albany NY)* **14**, 10050 (2022).
15. Kao, Y. et al. Shugoshin 2 is a biomarker for pathological grading and survival prediction in patients with gliomas. *Sci. Rep.* **11**, 18541 (2021).
16. Mossaid, I. & Fahrenkrog, B. Complex commingling: nucleoporins and the spindle assembly checkpoint. *Cells* **4**, 706–725 (2015).
17. Orth, M. et al. Shugoshin is a mad1/cdc20-like interactor of mad2. *The EMBO journal* **30**, 2868–2880 (2011).
18. Sotillo, R., Schvartzman, J.-M., Socci, N. D. & Benezra, R. Mad2-induced chromosome instability leads to lung tumour relapse after oncogene withdrawal. *Nature* **464**, 436–440 (2010).
19. Amin, M. B. *et al. AJCC cancer staging manual* (8th ed.). New York: Springer; 2017.
20. Wu, Z. et al. High sgo2 predicted poor prognosis and high therapeutic value of lung adenocarcinoma and promoted cell proliferation, migration, invasion, and epithelial-to-mesenchymal transformation. *J. Cancer* **14**, 2301 (2023).
21. Chen, Y. & Xiang, T. Sgo2 as a prognostic biomarker correlated with cell proliferation, migration, invasion, and epithelial-mesenchymal transition in lung adenocarcinoma. *Front. Biosci. (Landmark)* **29**, 314 (2024).
22. Sun, Q. et al. Shugoshin regulates cohesin, kinetochore-microtubule attachments, and chromosomal instability. *Cytogenet. Genome Res.* **162**, 283–296 (2023).
23. Michor, F., Iwasa, Y., Vogelstein, B., Lengauer, C. & Nowak, M. A. Can chromosomal instability initiate tumorigenesis?. *Semin. Cancer Biol.* **15**, 43–49 (2005).
24. Nowak, M. A. et al. The role of chromosomal instability in tumor initiation. *Proceedings of the National Academy of Sciences* **99**, 16226–16231 (2002).
25. Uhlmann, F. & Nasmyth, K. Cohesion between sister chromatids must be established during dna replication. *Current Biology* **8**, 1095–1102 (1998).
26. Riedel, C. G. et al. Protein phosphatase 2a protects centromeric sister chromatid cohesion during meiosis i. *Nature* **441**, 53–61 (2006).
27. Kitajima, T. S., Kawashima, S. A. & Watanabe, Y. The conserved kinetochore protein shugoshin protects centromeric cohesion during meiosis. *Nature* **427**, 510–517 (2004).
28. Tang, Z. et al. Pp2a is required for centromeric localization of sgo1 and proper chromosome segregation. *Dev. Cell* **10**, 575–585 (2006).
29. Uhlmann, F., Lottspeich, F. & Nasmyth, K. Sister-chromatid separation at anaphase onset is promoted by cleavage of the cohesin subunit scc1. *Nature* **400**, 37–42 (1999).
30. Hellmuth, S., Gómez-H, L., Pendás, A. M. & Stemmann, O. Securin-independent regulation of separase by checkpoint-induced shugoshin-mad2. *Nature* **580**, 536–541 (2020).
31. Yao, Y. & Dai, W. Shugoshins function as a guardian for chromosomal stability in nuclear division. *Cell Cycle* **11**, 2631–2642 (2012).
32. Liu, S. et al. Mad2 promotes cyclin b2 recruitment to the kinetochore for guiding accurate mitotic checkpoint. *EMBO reports* **23**, e54171 (2022).
33. Khot, M. et al. Twist1 induces chromosomal instability (cin) in colorectal cancer cells. *Hum. Mol. Genet.* **29**, 1673–1688 (2020).
34. Carstens, J. L. & Lovisa, S. Epithelial-to-mesenchymal transition drives cancer genomic instability. *J. Exp. Clin. Cancer Res.* **44**, 135 (2025).

Acknowledgements

I would like to express my heartfelt gratitude to Director Chuandong Zhu and Director Huihui Zhao for their guidance on this manuscript. My sincere thanks also go to Wenzheng Zhou and Guohao Wei for their assistance with my experiments, as well as to Mengyao Lü and Yan Sun for their support and help.

Author contributions

The authors contributed to the study as follows: Min Sun carried out the majority of the experiments and prepared the manuscript draft. Wenzheng Zhou and Guohao Wei were responsible for data analysis. Mengyao Lü and Yan Sun collected clinical samples. Chuandong Zhu and Huihui Zhao provided guidance for the experiments and manuscript writing.

Funding

This study was funded by Medical science and technology development project of Nanjing (YKK22130, ZKX23037), Natural science Fund projects of Nanjing University of Chinese Medicine (XZR2021080), Talent lift Fund projects of Nanjing Second Hospital (RCMS23006, RCZD202302), General Project of the National Health Commission's Special Research Fund for Post-Marketing Clinical Studies of Innovative Drugs (WKZX-2024CX101211) and Wu Jieping Medical Foundation Clinical Research Special Grant (320.6750.2023-17-2).

Declarations

Competing interests
The authors declare no competing interests.

Ethics statement
The studies involving humans were approved by Nanjing Second Hospital Scientific and Ethical (Review) Committee. The research was carried out in compliance with local laws and institutional guidelines. Written informed consent was obtained from all participants for their involvement in the study.

Additional information
Supplementary Information The online version contains supplementary material available at https://doi.org/10.1038/s41598-025-10993-0.

Correspondence and requests for materials should be addressed to H.Z. or C.Z.

Reprints and permissions information is available at www.nature.com/reprints.

Publisher's note Springer Nature remains neutral with regard to jurisdictional claims in published maps and institutional affiliations.